



## A BNAIP-heterocycle†

 Tim Wellnitz,<sup>ab</sup> Leonie Wüst,<sup>ab</sup> Holger Braunschweig<sup>ib</sup>\*<sup>ab</sup> and Christian Hering-Junghans<sup>id</sup>\*<sup>c</sup>

 Cite this: *Chem. Commun.*, 2025, 61, 4014

 Received 17th January 2025,  
 Accepted 5th February 2025

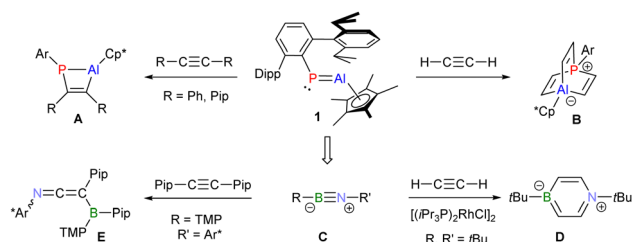
DOI: 10.1039/d5cc00308c

rsc.li/chemcomm

We report the [2+2]-cyclization reaction of a phosphaalumene with its lighter analog, an iminoborane, to give a species with a four-membered BNAIP-heterocycle with alternating Lewis basic and acidic centers in the ring. The reactivity of this heterocycle towards alkenes and alkynes is described, giving chain molecules and ring-expanded species.

Multiple bonds of heavier main group elements<sup>1</sup> are the focus of contemporary research for their potential in the activation of small, unreactive molecules, the design of new materials, and for their potential applications in catalysis.<sup>2,3</sup> Among these, Pn–Al (Pn = P, As) multiple bonds have long evaded synthetic realization.<sup>4</sup> In 2021 the first phospho- and arsaaluminenes were synthesized as thermally robust, violet or blue crystalline compounds,<sup>5</sup> respectively, with a strongly shielded <sup>31</sup>P NMR signal in the phosphaalumene. <sup>D1pp</sup>TerPn = AlCp\* (Pn = P (1), As; <sup>D1pp</sup>Ter = 2,6-(2,6-*i*Pr<sub>2</sub>C<sub>6</sub>H<sub>3</sub>)-C<sub>6</sub>H<sub>3</sub>) show *E*-configured Pn–Al multiple bonds, which are strongly polarized towards the pnictogen center, especially the  $\pi$ -component. Despite its strong polarization the P–Al bond in **1** readily engages in [2+2]-cycloaddition reactions, for example with disubstituted alkynes, giving so-called 1,2-phosphaaluminetes (Scheme 1, A). With acetylene two additional molecules insert into the P–Al bond giving 1,4-phosphaaluminabarrelenes (Scheme 1, B).<sup>6</sup> Iminoboranes of the general form R–N $\equiv$ B–R' are isosters of alkynes and are the isovalence electronic lighter analogs of **1**. The triple bond character in iminoboranes differs from phosphaborenes,<sup>7,8</sup> -aluminenes<sup>5,9</sup> and -gallenes<sup>10–13</sup> with negligible non-classical triple bond character.

By contrast to alkynes the B $\equiv$ N bond in iminoboranes is strongly polarized (similar to **1**); thus, its chemistry is dominated by oligomerization processes. Steric protection, or Lewis bases can significantly stabilize the B $\equiv$ N bond and suppress oligomerization.<sup>14</sup> The parent iminoborane HNBH has only been stabilized in push–pull fashion through FLP-type stabilization.<sup>15</sup> *t*Bu–N $\equiv$ B–*t*Bu (Scheme 1, C) is a moderately stable variant (*t*<sub>1/2</sub> at 50 °C *ca.* 3 d) and was shown to engage in dipolar [3+2]-cycloaddition reactions with organic azides and diazomethane derivatives even at low temperatures.<sup>16</sup> In the coordination sphere of rhodium, *t*Bu–N $\equiv$ B–*t*Bu has been shown to selectively react with alkynes to give 1,2- and 1,4-azaborinines (Scheme 1, D).<sup>17–19</sup> In the case of 1,4-azaborinines this process involves B $\equiv$ N bond scission, which has also been observed in the reaction of *t*Bu–N $\equiv$ B–*t*Bu with silylenes or when the sterically crowded iminoborane (TMP)B $\equiv$ NAr\* (Scheme 1, E; TMP = 2,2,6,6-tetramethylpyrrolidyl; Ar\* = 2,6-(Ph<sub>2</sub>CH)-4-*t*Bu-C<sub>6</sub>H<sub>2</sub>) reacted with the activated alkyne C<sub>2</sub>Pip<sub>2</sub> (Pip = piperidyl).<sup>20</sup> In this study we investigate the reactivity of phosphaalumene **1** towards its formal “smaller sibling” iminoborane *t*Bu–N $\equiv$ B–*t*Bu, giving the first example of a four-membered ring containing B, N, Al and P. This ring species was further treated with alkenes and alkynes, revealing insertion into the P–B-bond, in stark contrast to previously reported PAIC<sub>2</sub>-ring species.



**Scheme 1** Reactivity of phosphaalumene <sup>D1pp</sup>TerPAICp\* (**1**) and iminoboranes (C) towards different alkynes (TMP = 2,2,6,6-tetramethylpyrrolidyl; Pip = piperidyl; Ar\* = 2,6-(Ph<sub>2</sub>CH)-4-*t*Bu-C<sub>6</sub>H<sub>2</sub>).

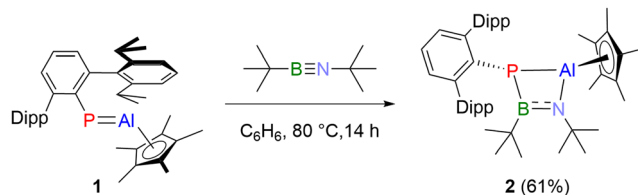
<sup>a</sup> Institute for Inorganic Chemistry, Julius-Maximilians-Universität Würzburg, Am Hubland, 97074 Würzburg, Germany. E-mail: h.braunschweig@uni-wuerzburg.de

<sup>b</sup> Institute for Sustainable Chemistry & Catalysis with Boron, Julius-Maximilians-Universität Würzburg, Am Hubland, 97074 Würzburg, Germany

<sup>c</sup> Leibniz Institute for Catalysis e.V. (LIKAT), A.-Einstein-Str. 29a, 18059 Rostock, Germany. E-mail: christian.hering-junghans@catalysis.de

† Electronic supplementary information (ESI) available: Synthesis and characterization of compounds, NMR spectra, crystallographic, and computational details. CCDC 2417544–2417546. For ESI and crystallographic data in CIF or other electronic format see DOI: <https://doi.org/10.1039/d5cc00308c>



Scheme 2 Synthesis of BNAIP heterocycle **2**.

When **1** and  $t\text{Bu-N}\equiv\text{B-tBu}$  were combined in benzene no immediate reaction was detected (Scheme 2), however after heating at 80 °C for 14 h the characteristic violet color of **1** had faded into a dull yellow to green solution. NMR spectroscopy revealed full conversion of **1** and formation of a new species with a rather sharp singlet in the  $^{31}\text{P}$  NMR spectrum at  $-59.9$  ppm (*cf.*  $(\text{Mes}^*\text{P}(\text{H}_2\text{CO})\text{BTmp})_2$ ,  $\delta(^{31}\text{P}) = -61.0$  ppm)<sup>21</sup> and a broad singlet at 56.0 ppm in the  $^{11}\text{B}$  NMR spectrum, indicating a three-coordinate boron atom. Single crystal X-ray diffraction (SCXRD) experiments revealed the formation of compound **2** (Fig. 1), a species with a BNAIP four-membered ring, which can be classified as *cyclo*-1-alumina-3-borata-4-phospha-2-azene. **2** is the product of a formal [2+2]-cycloaddition between **1** and  $t\text{Bu-N}\equiv\text{B-tBu}$  with the expected P,B- and Al,N-connectivity and a puckered ring (P1–B1–N1–Al1 13.21(9)°) with the substituents on P and Al being minimally *trans*-oriented with respect to the P–Al axis.

The B ( $\sum(\angle\text{B}) = 356.62^\circ$ ) and N ( $\sum(\angle\text{N}) = 358.86^\circ$ ) atoms are in distorted trigonal planar coordination environments with a short B–N distance (1.425(2) Å) as expected for aminoboranes (*cf.*  $\sum r_{\text{cov}}(\text{B}=\text{N}) = 1.38$  Å;<sup>22</sup> (IDipp)(Mes)B=N(*t*Bu)Dipp 1.420(2) Å).<sup>23</sup> The Cp\*–substituent is  $\eta^5$ -coordinated to an aluminium atom that deviates from an ideal trigonal planar coordination ( $\Sigma(\angle\text{Al}) = 349.5^\circ$ ) with Al–N (1.8751(12) Å) and Al–P (2.3380(5) Å) distances that are in line with polarized single bonds (*cf.*  $\sum r_{\text{cov}}(\text{Al-P}) = 2.37$ , (Al–N) = 1.97 Å).<sup>22</sup> The phosphorus atom is trigonal pyramidally coordinated with a rather long P–B distance (2.005(2) Å; *cf.*  $\text{Mes}^*\text{P}(\text{PhCCH})\text{B}(\text{TMP})$ <sup>24</sup> 1.987(2) Å). According to NBO analysis

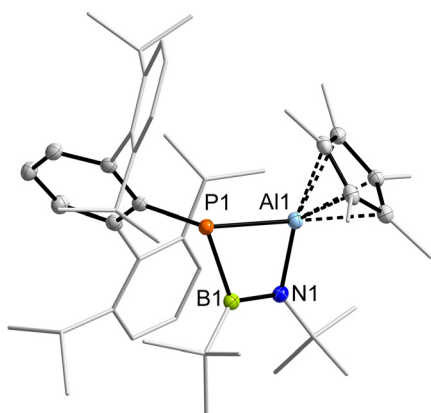
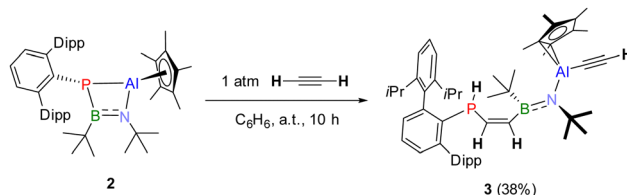


Fig. 1 Molecular structure of **2**. Ellipsoids drawn at 50% probability with C–H-atoms omitted, Dipp-, *t*Bu- and Me-groups of Cp\* rendered as wire-frame for clarity. Selected bond lengths [Å] and angles [°]: P1–Al1 2.3380(5), P1–B1 2.005(2), B1–N1 1.425(2), N1–Al1 1.875(1); B1–P1–Al1 69.66(5), P1–B1–N1 108.4(1), B1–N1–Al1 97.30(9), P1–Al1–N1 82.64(4); P1–B1–N1–Al1 13.21(9).

Scheme 3 Reactivity of **2** towards acetylene.

at the PBE0-D3/def2-TZVP level of theory the P–B bond is delocalized into a lone valence (LV) at the aluminium center, which is further accepting electron density from a p-type lone pair of electrons on the nitrogen atom, as well as from the s-type LP at the P center. This results in a ring with alternating natural charges (P:  $-1.28$ ; Al 1.79; N  $-1.28$ ; B 0.85 *e*) and Wiberg Bond Indexes that are in line with polarized single bonds (P–Al 0.65, N–Al 0.30, P–B 0.97), with a high ionic character in the case of the Al–N bond. The B–N bond is strongly polarized towards the N atom ( $\sigma$  81%,  $\pi$  85%), thus resulting in a WBI close to one (B–N 1.04). Next the reactivity of **2** towards C–C multiple bond systems was investigated. As a first entry a benzene solution of **2** was stirred under an atmosphere of  $\text{C}_2\text{H}_2$  for 1 h (Scheme 3), which, according to  $^{31}\text{P}$  NMR spectroscopy, resulted in the formation of a mixture of products ( $\delta(^{31}\text{P}) = -73.0$  (16%),  $-78.1$  (67%),  $-81.0$  (16%) ppm), while in the  $^{11}\text{B}$  NMR spectrum a broad singlet at 50.4 ppm was detected.

SCXRD-quality crystals were obtained by slow evaporation of a saturated *n*-pentane solution, which revealed formation of the chain-molecule  $^{\text{Dipp}}\text{TerP}(\text{H})\text{-C}(\text{H})=\text{C}(\text{H})\text{-B}(\text{tBu})\text{-N}(\text{tBu})\text{-Al}(\eta^5\text{-Cp}^*)(\text{C}\equiv\text{CH})$  (**3**) (Fig. 2). We hypothesize that **3** results from initial acetylene insertion into the strongly polarized P–B bond (Fig. S31, ESI<sup>†</sup>), with subsequent deprotonation of acetylene by the P atom and Al capturing the released acetylenide anion resulting in P–Al bond cleavage. A reverse order of addition, first across the P–Al bond with C–H bond cleavage and subsequent insertion of the second  $\text{C}_2\text{H}_2$  into the P–B bond cannot be ruled out. The presence of three different isomers in solution is due to conformers of the alternating C=C (1.338(3) Å) and B=N (1.408(3) Å)

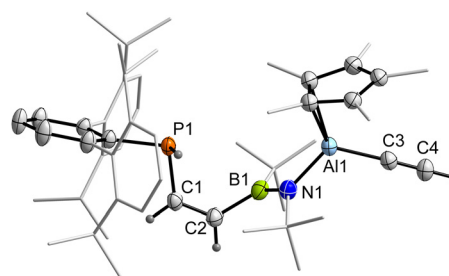


Fig. 2 Molecular structure of **3**. Ellipsoids drawn at 50% probability with C–H-atoms omitted (except on P1, C1, C2, C4), Dipp-, *t*Bu- and Me-groups of Cp\* rendered as wire-frame for clarity. Selected bond lengths [Å] and angles [°]: P1–C1 2.3380(5), C1–C2 1.338(3), C2–B1 1.612(3), B1–N1 1.408(3), N1–Al1 1.855(2), N1–Al1 1.855(2), Al1–C3 1.919(2), C3–C4 1.198(3); P1–C1–C2 120.8(1), C1–C2–B1 125.8(2), C2–B1–N1 123.7(2), B1–N1–Al1 123.6(1), N1–Al1–C3 116.34(8), Al1–C3–C4 176.3(2); C1–C2–B1–N1 96.5(3), P1–C1–C2–B1  $-7.0(3)$ , C2–B1–N1–Al1  $-158.81(15)$ .



double bonds, with the *Z*(CC)/*E*(BN) isomer being present in the solid state. This reactivity clearly differs from **1**, which reacted with acetylene through threefold insertion into the P–Al bond.<sup>6</sup>

The conjugated C=C–B=N unit is terminated by P–C (1.821(2) Å) and N–Al (1.855(2) Å) single bonds. The B ( $\sum(\angle B) = 359.4^\circ$ ), N ( $\sum(\angle N) = 360.0^\circ$ ) and Al ( $\sum(\angle Al) = 357.6^\circ$ ) atoms are distorted trigonally planar coordinated with a terminal C≡CH unit (the asymmetric CH stretching vibration is detected in the IR at 3258 cm<sup>-1</sup>) on the Al atom ( $d(C3-C4) = 1.198(3)$  Å) and an  $\eta^2$ -coordinated Cp\*-substituent ( $d(Al-C_{Cp^*}) = 2.120(2), 2.133(2)$  Å). Interestingly, the trigonal pyramidal P atom ( $\sum(\angle P) = 301.0^\circ$ ) is protonated. In the <sup>1</sup>H NMR spectrum of **3** the main isomer can be clearly characterized with a ddd-signature for the P–CH proton at 6.80 ppm and a doublet at 6.38 ppm for the B–CH proton, while the P–H gives a doublet of doublets at 4.40 ppm ( $J_{PH} = 226.6$  Hz,  $^3J_{PH} = 2.6$  Hz) and the terminal CCH proton is detected as a singlet at 1.59 ppm. <sup>1</sup>H DOSY experiments revealed similar diffusion coefficients for all three isomers detected in the <sup>31</sup>P NMR spectrum, supporting the notion that these only differ in the configuration of the double bonds.

When **1** was treated with an excess of styrene at ambient temperature in C<sub>6</sub>D<sub>6</sub> no reaction occurred. Heating to 80 °C for at least 2 days, gave three new signals in the <sup>31</sup>P NMR spectrum at –10.4, –19.3 and –20.9 ppm, which correspond to the different regio-isomers of twofold styrene insertion into the P–Al bond in **1**, giving 1,4-aluminaphosphorinanes (**5**, Scheme 5), which we had previously reported.<sup>6</sup> The <sup>11</sup>B NMR spectrum of the reaction mixture clearly indicated the release of *t*BuN≡B*t*Bu, foreshadowing that **2** can act as a disguised form of **1**. When first treating <sup>D</sup>IPP<sub>2</sub>TerPAlCp\* with styrene (1.6 eq.), giving the previously reported phosphaalumate **1<sup>Ph</sup>** *in situ* (Scheme 4),<sup>6</sup> followed by the addition of *t*Bu–N≡B–*t*Bu (1 eq.) the formation of a new species with a <sup>31</sup>P NMR signal at –39.2 ppm was detected, shielded compared to **1<sup>Ph</sup>** (*cf.*  $\delta(^{31}P) = 76.0$  ppm).<sup>6</sup> SCXRD experiments revealed the formation of a six-membered PC<sub>2</sub>BNAl-heterocycle (**4**, Fig. 3), formed through insertion of the iminoborane into the Al–C bond in **1<sup>Ph</sup>**. The six-membered ring shows an envelope conformation, being folded *ca.* 115° along the Al1–C1 axis. Both the P1–C2 (1.908(1) Å) and P1–Al1 (2.3695(4) Å) distances are similar to those in **1<sup>Ph</sup>** (*cf.* 1.920(1), 2.3992(5) Å),<sup>6</sup> with the Al1–N1 (1.842(1) Å) distance being minimally shorter compared to **2**. The Al atom is in a distorted trigonal planar coordination environment with an  $\eta^1$ -coordinated Cp\*-substituent ( $d(Al1-C17) 2.044(1)$  Å). The C2–C1 (1.575(2) Å) and C1–B1 distances (1.654(2) Å) are also in line with single bonds (*cf.*  $\sum r_{cov}(B-C) = 1.60, (C-C) = 1.50$  Å),<sup>22</sup> while the N1–B1 (1.403(2) Å) is

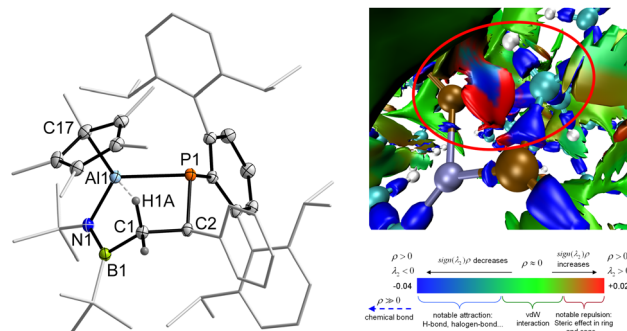
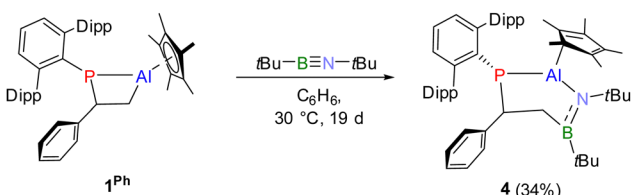


**Fig. 3** Molecular structure of **4** (left). Ellipsoids drawn at 50% probability with C–H-atoms omitted (except on C1, C2, with HAR refinement), Dipp-, *t*Bu-, Ph- and Me-groups of Cp\* rendered as wire-frame for clarity. Selected bond lengths [Å] and angles [°]: P1–C2 1.908(1), C1–C2 1.575(2), C1–B1 1.653(2), B1–N1 1.403(2), N1–Al1 1.8445(9), Al1–P1 2.3695(4), Al1–C1 1.2294(1), Al1–C17 2.044(1), C1–H1A 1.133(14); P1–C2–C1 105.78(8), C2–C1–B1 114.1(1), C1–B1–N1 111.9(1), B1–N1–Al1 97.68(9), N1–Al1–P1 116.23(4), Al1–H1A–C1 89.1(8); Al1–N1–B1–C1 116.23(4), Al1–C1–C2–P1 18.26(8). Illustration of the results from an IRI-analysis at the PBE0-D3/def2-TZVP level of theory (right), with the corresponding Al–CH interaction circled in red (Al: brown; C: turquoise; H: white).

similar to that in **2** and in line with the formulation of **4** as a cyclic aminoborane, which is further corroborated by the BN stretching vibration at 1361 cm<sup>-1</sup> in the IR spectrum.

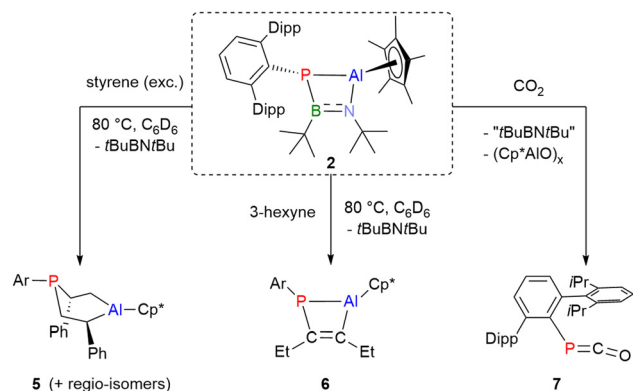
In solution the description of **4** as a cyclic aminoborane is supported by a broad singlet in the <sup>11</sup>B NMR spectrum (tol-*d*<sub>8</sub>) at 44.5 ppm. The <sup>1</sup>H NMR spectrum of **4** is complex, indicating C<sub>1</sub> symmetry in solution. A singlet for the Cp\* substituent indicates a fast sigmatropic rearrangement in solution, while two characteristic signals for the diastereotopic ring CH<sub>2</sub> protons are detected at –0.41 and *ca.* 1.55 ppm. Compared to **1<sup>Ph</sup>** (PhCHCH<sub>2</sub>  $\delta(^1H) = 1.76, 2.04$  ppm) one of the CH<sub>2</sub> protons is significantly shielded (–0.41 ppm) with a complex coupling pattern, that also includes through space  $J_{PH}$  coupling (6.8 Hz). This shielding is indicative of an agostic interaction of the C–H bond with the Al center.<sup>25</sup> This is further supported by a short C1–Al1 distance (2.294(1) Å) and an Al1···H–C1 angle of 89.1(8)° determined with Hirshfeld atom refinement (HAR).<sup>26</sup> 2nd order perturbation theory analysis at the PBE0-D3/def2-TZVP level of theory reveals a donor–acceptor interactions between the C–H bond and a lone valence at aluminium of *ca.* 26 kcal mol<sup>-1</sup>. This significant interaction is further supported by an interaction region indicator (IRI) analysis (Fig. 3, right).<sup>27</sup> Interestingly, when a C<sub>6</sub>D<sub>6</sub> solution of **4** was heated to 60 °C the formation of **2** was detected with release of styrene.

Additionally, the reactivity of **2** towards 3-hexyne was probed. To *in situ* generated **2** in C<sub>6</sub>D<sub>6</sub>, 3-hexyne was added and the mixture was heated at 80 °C for 24 h, showing partial conversion of **2** into a new species with a <sup>31</sup>P NMR signal at 40.6 ppm with the concomitant release of *t*BuN≡B*t*Bu. This indicated the formation of a four-membered species, phosphaalumate <sup>D</sup>IPP<sub>2</sub>TerP(EtC=CeT)AlCp\* (**6**, Scheme 5), by comparison with the <sup>31</sup>P NMR shifts of previously reported derivatives (*cf.* <sup>D</sup>IPP<sub>2</sub>TerP(PhC=CPh)AlCp\* 35.3 ppm).<sup>6</sup> A rather clean reaction was observed when a *n*-pentane solution of **2** was



**Scheme 4** Synthesis of six-membered heterocycle **4**.





Scheme 5 Reactivity of **2** towards excess of styrene, 3-hexyne and CO<sub>2</sub>.

exposed to CO<sub>2</sub>, resulting in a color change to orange. A singlet in the <sup>31</sup>P NMR spectrum at –201.8 ppm shows conversion into the previously reported phosphaketene <sup>Dipp</sup>TerPCO (**7**, Scheme 5),<sup>12</sup> while a broad signal in the <sup>11</sup>B NMR spectrum at ca. 36 ppm indicated further reaction of the iminoborane with CO<sub>2</sub> to an unidentified product, along with signals for oligomeric [Cp\*AlO]<sub>x</sub> in the <sup>1</sup>H NMR spectrum.<sup>28</sup> These reactivities underline that **2** in some cases acts as a disguised source of **1**.

In summary the synthesis of the unique BNAIP heterocycle **2** has been described. While **2** reacted with acetylene *via* insertion into the P–B bond to give conjugated aminoborane **3**, the reaction with styrene resulted in iminoborane release. However, when the order of addition was changed the 6-membered aminoborane **4** was afforded, which shows an intramolecular agostic Al··(C–H) interaction. Studies harnessing the lability of the *t*BuNB*t*Bu unit in **2** are currently underway. Moreover, the reactivity of **2** towards E–H bonds (E = H, B, Si, N, *etc.*) will be explored, as well as that of aryl phosphaketene <sup>Dipp</sup>TerPCO.

T. W. designed and carried out the experimental work, collected and analysed the data and assembled the ESI.† T. W. and L. W. carried out the SCXRD experiments. T. W. and C. H.-J. did the DFT calculations. H. B. and C. H.-J. supervised the work and drafted the manuscript. All authors have given approval to the final version of the manuscript.

C. H.-J. wishes to thank the ITMZ at the University of Rostock for access to the Cluster Computer and especially Malte Willert for technical support. T. W. thanks Krzysztof Radacki for help with X-ray analysis and calculations. H. B. wishes to acknowledge financial support by the DFG.

## Data availability

The data supporting this article, including synthetic procedures, spectral data, and crystallographic and computational details have been included as part of the ESI.† Crystallographic

data has been deposited at the CCDC under identification numbers 2417544 (**2**), 2417545 (**3**) and 2417546 (**4**), respectively.

## Conflicts of interest

There are no conflicts to declare.

## Notes and references

- P. P. Power, *Organometallics*, 2020, **39**, 4127–4138.
- C. Weetman, *Chem. – Eur. J.*, 2021, **27**, 1941–1954.
- F. Hanusch, L. Groll and S. Inoue, *Chem. Sci.*, 2021, **12**, 2001–2015.
- F. Dankert and C. Hering-Junghans, *Chem. Commun.*, 2022, **58**, 1242–1262.
- M. Fischer, S. Nees, T. Kupfer, J. T. Goettel, H. Braunschweig and C. Hering-Junghans, *J. Am. Chem. Soc.*, 2021, **143**, 4106–4111.
- S. Nees, T. Wellnitz, F. Dankert, M. Härterich, S. Dotzauer, M. Feldt, H. Braunschweig and C. Hering-Junghans, *Angew. Chem., Int. Ed.*, 2023, **62**, e202215838.
- J. Li, Z. Lu and L. L. Liu, *J. Am. Chem. Soc.*, 2022, **144**, 23691–23697.
- E. A. LaPierre, B. O. Patrick and I. Manners, *J. Am. Chem. Soc.*, 2023, **145**, 7107–7112.
- L. S. Szych, L. Denker, J. Feld and J. M. Goicoechea, *Chem. – Eur. J.*, 2024, **30**, e202401326.
- D. W. N. Wilson, J. Feld and J. M. Goicoechea, *Angew. Chem., Int. Ed.*, 2020, **59**, 20914–20918.
- M. K. Sharma, C. Wölper, G. Haberhauer and S. Schulz, *Angew. Chem., Int. Ed.*, 2021, **60**, 6784–6790.
- T. Taeufer, F. Dankert, D. Michalik, J. Pospech, J. Bresien and C. Hering-Junghans, *Chem. Sci.*, 2023, **14**, 3018–3023.
- Á. García-Romero, C. Hu, M. Pink and J. M. Goicoechea, *J. Am. Chem. Soc.*, 2025, **147**, 1231–1239.
- Y. Fan, J. Cui and L. Kong, *Eur. J. Org. Chem.*, 2022, e202201086.
- (a) A. K. Swarnakar, C. Hering-Junghans, K. Nagata, M. J. Ferguson, R. McDonald, N. Tokitoh and E. Rivard, *Angew. Chem., Int. Ed.*, 2015, **54**, 10666–10669; (b) B. L. Frenette, A. A. Omana, M. J. Ferguson, Y. Zhou and E. Rivard, *Chem. Commun.*, 2021, **57**, 10895–10898.
- P. Paetzold, C. V. Plotho, G. Schmid, R. Boese, B. Schrader, D. Bougeard, U. Pfeiffer, R. Gleiter and W. Schüfer, *Chem. Ber.*, 1984, **117**, 1089–1102.
- H. Braunschweig, K. Geetharani, J. O. C. Jiménez-Halla and M. Schäfer, *Angew. Chem., Int. Ed.*, 2014, **53**, 3500–3504.
- M. Heß, I. Kruppenacher, T. Dellermann and H. Braunschweig, *Chem. – Eur. J.*, 2021, **27**, 9503–9507.
- M. Schäfer, N. A. Beattie, K. Geetharani, J. Schäfer, W. C. Ewing, M. Krahuß, C. Hörl, R. D. Dewhurst, S. A. Macgregor, C. Lambert and H. Braunschweig, *J. Am. Chem. Soc.*, 2016, **138**, 8212–8220.
- L. Winner, A. Hermann, G. Bélanger-Chabot, O. F. González-Belman, J. O. C. Jiménez-Halla, H. Kelch and H. Braunschweig, *Chem. Commun.*, 2018, **54**, 8210–8213.
- A. M. Borys, E. F. Rice, G. S. Nichol and M. J. Cowley, *J. Am. Chem. Soc.*, 2021, **143**, 14065–14070.
- P. Pyykkö and M. Atsumi, *Chem. – Eur. J.*, 2009, **15**, 12770–12779.
- L. Winner, G. Bélanger-Chabot, M. A. Celik, M. Schäfer and H. Braunschweig, *Chem. Commun.*, 2018, **54**, 9349–9351.
- A. N. Price, G. S. Nichol and M. J. Cowley, *Angew. Chem., Int. Ed.*, 2017, **56**, 9953–9957.
- M. Brookhart, M. L. H. Green and G. Parkin, *Proc. Nat. Acad. Sci. U. S. A.*, 2007, **104**, 6908–6914.
- F. Kleemiss, O. V. Dolomanov, M. Bodensteiner, N. Peyerimhoff, L. Midgley, L. J. Bourhis, A. Genoni, L. A. Malaspina, D. Jayatilaka, J. L. Spencer, F. White, B. Grundkötter-Stock, S. Steinbauer, D. Lentz, H. Puschmann and S. Grabowsky, *Chem. Sci.*, 2021, **12**, 1675–1692.
- T. Lu and Q. Chen, *Chem.: Methods*, 2021, **1**, 231–239.
- A. C. Stelzer, P. Hrobárik, T. Braun, M. Kaupp and B. Braun-Cula, *Inorg. Chem.*, 2016, **55**, 4915–4923.

